Electron Transfer

DOI: 10.1002/anie.200605039

Tuning Electron Transfer through Translational Motion in Molecular Shuttles**

Aurelio Mateo-Alonso, Christian Ehli, G. M. Aminur Rahman, Dirk M. Guldi,* Giulia Fioravanti, Massimo Marcaccio, Francesco Paolucci,* and Maurizio Prato**

Rapid advances in our ability to construct, image, manipulate, and probe properties of matter at the atomic scale—together with emerging insights into structure, function, and self-assembly in biological systems—allow the construction of systems that will ultimately execute precise functions over several atomic diameters. A prototype of such molecular machines[1] integrates two major constituents into a single, atomically precise system: a moveable and a stationary part. The moveable component should be reversibly displaceable, with respect to the stationary part, through the application of an external stimulus. As in macroscopic machines, such a displacement should put together or place apart two different counterparts and, in turn, execute predetermined tasks.

A versatile molecular approach relies on the accomplishments in the field of interlocked architectures, in which rotaxanes have emerged among the most promising candidates. Rotaxanes comprise a molecular axle that is threaded through a macrocyclic ring. The macrocycle is trapped by means of two bulky stoppers. Controlled translocation of the macrocycle (shuttling) between different parts of the thread (stations) can be achieved by applying stimuli that range from illumination[2,3] and variation of the electrochemical potential[4–6] to solvent[7–10] or pH change.[11,12] An area that has found little attention is the implementation of molecular shuttles into light-driven electron-transfer systems. Particularly intriguing is the control over the reversible activation/deactivation of the energy-converting electron-transfer process. The opportunities that will emerge when combining molecular shuttling and solar-energy conversion remain, to the best of our knowledge, unexplored.

Herein, we report on a molecular shuttle in which a large positional change of the macrocycle (bearing two ferrocene groups as electron donors) along the thread (functionalized with a fullerene electron acceptor) is used to modulate/fine-tune the kinetics of intraensemble charge separation and recombination. Two rotaxanes were carefully designed and synthesized to explore the impact of molecular shuttling on electronic communication between the photo- and electroactive constituents (Scheme 1). In rotaxane **2**, the relative position of the macrocycle (and those of the donor and the acceptor) along the thread is fixed, independently of the solvent used. In contrast, in rotaxane **5**, the macrocycle can be positioned close to or far from the fullerene, depending on the solvent used (see below). Charge-transfer rates and efficiencies in the different translational isomers of **5** are evaluated by direct comparison with rotaxane **2**. Consequently, any effect observed is undoubtedly owed to the relative position of the donor and the acceptor and not related to the solvent.

Thread **1** comprises a fullerene, a diphenyl stopper, and a fumaramide template (Scheme 1).[13] To increase the solubility of thread **1** in organic solvents, an alkyl chain was introduced through 1,3-dipolar cycloaddition.[14,15] Rotaxane **2** was assembled using a modification of the protocol developed by Leigh and co-workers for the preparation of benzilic amide rotaxanes[16] by using 5-ferroceneacetoxyisophthaloyl chloride (**3**). The excellent arrangement and rigidity of the hydrogen-bond recognition sites endow the fumaramide groups with a strong affinity for the macrocycle, even in solvents of high hydrogen-bond basicity (for example, dimethyl sulfoxide, DMSO).[16–18] The strong macrocycle–template interactions, together with the short length of thread **1**, ensure that the macrocycle sits over the template. The ^{1}H NMR spectrum of rotaxane **2** shows the typical features of a fumaramide rotaxane[16] (Figure 1a,b). Protons B (the assignments correspond to those shown in Scheme 1) are shielded by the benzylic amide rings of the macrocycle relative to the protons of thread **1**, thus confirming that the macrocycle is positioned over the fumaramide template.

Rotaxane **5** was assembled from thread **4** by using the procedure applied for the preparation of rotaxane **2** (Scheme 1). Thread **4** comprises a fullerene stopper attached

[*] Dr. A. Mateo-Alonso, Prof. M. Prato
Italian Interuniversity Consortium on Materials, Science, and Technology (INSTM), Unit of Trieste
Dipartimento di Scienze Farmaceutiche, Università di Trieste
Piazzale Europa 1, 34127 Trieste (Italy)
Fax: (+39) 040-52572
E-mail: amateo@units.it
prato@units.it
C. Ehli, Dr. G. M. A. Rahman, Prof. D. M. Guldi
Lehrstuhl für Physikalische Chemie I
Universität Erlangen-Nürnberg
Egerlandstrasse 3, 91058 Erlangen (Germany)
Fax: (+49) 9131-852-8307
E-mail: guldi@chemie.uni-erlangen.de
Dr. G. Fioravanti, Dr. M. Marcaccio, Prof. F. Paolucci
Dipartimento di Chimica "G. Ciamician"
Università di Bologna, v. Selmi 2, 40126 Bologna (Italy)
Fax: (+39) 051-209-9456
E-mail: francesco.paolucci@unibo.it

[**] We thank Prof. David A. Leigh for helpful discussions and for introducing us to this field. This work was carried out with partial support from the University of Trieste, INSTM, MIUR (PRIN 2006, prot. 20064372 and Firb, prot. RBNE033KMA), the EU (RTN networks "WONDERFULL" and "EMMMA"), the Deutsche Forschungsgemeinshaft (SFB 583), FCI, and the Office of Basic Energy Science of the US Department of Energy (NDRL 4717).

Supporting information for this article is available on the WWW under http://www.angewandte.org or from the author.

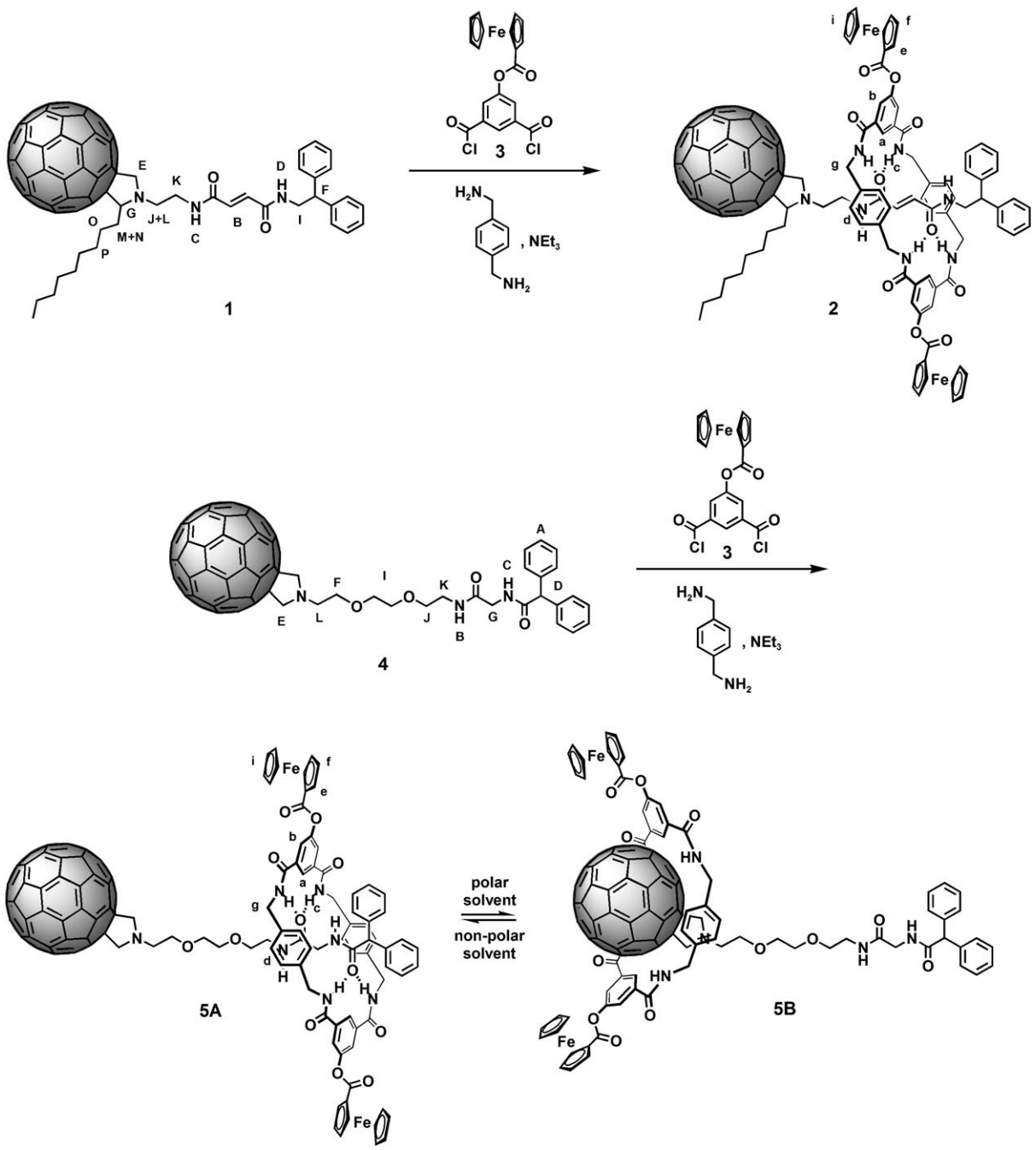

Scheme 1. Structure and behavior of the fullerene–ferrocene dyads.

to a peptidic template (which contains a diphenyl stopper) through a triethyleneglycol spacer. The dipeptide possesses a moderate affinity for the macrocycle, relative to the fumaramide, since the hydrogen-bonding sites are not rigid and intramolecular hydrogen bonds may form.[16] The macrocycle can be decomplexed from the dipeptide by changing to a highly polar solvent, which solvates the hydrogen-bonding sites of the macrocycle and the peptide more strongly than they bind to each other.[7,8,10] In fact, rotaxane **5** exists in two different co-conformations in different solvents (see Figure 1, and Figures S1 and S2 in the Supporting Information). In relatively nonpolar solvents (for example, CD_2Cl_2, $CDCl_3$), protons G, C, and D (Figure 1 c, d) are shielded relative to the protons of thread **4**, thereby confirming that the macrocycle is located primarily over the peptidic residue (co-conformer **5A**), while in highly polar solvents (for example, [D_7]DMF and [D_6]DMSO, DMF = *N*,*N*-dimethylformamide), the hydrogen bonds are weakened, thereby promoting the formation of π-stacking interactions between the macrocycle and the fullerene. Therefore, the macrocycle shuttles to the opposite end of the thread, preferentially adopting the stacked co-conformation **5B**, which is reflected by shielding of protons E, L, and F (Figure 1 e, d). The discrimination for the different stations is less well expressed in solvents with

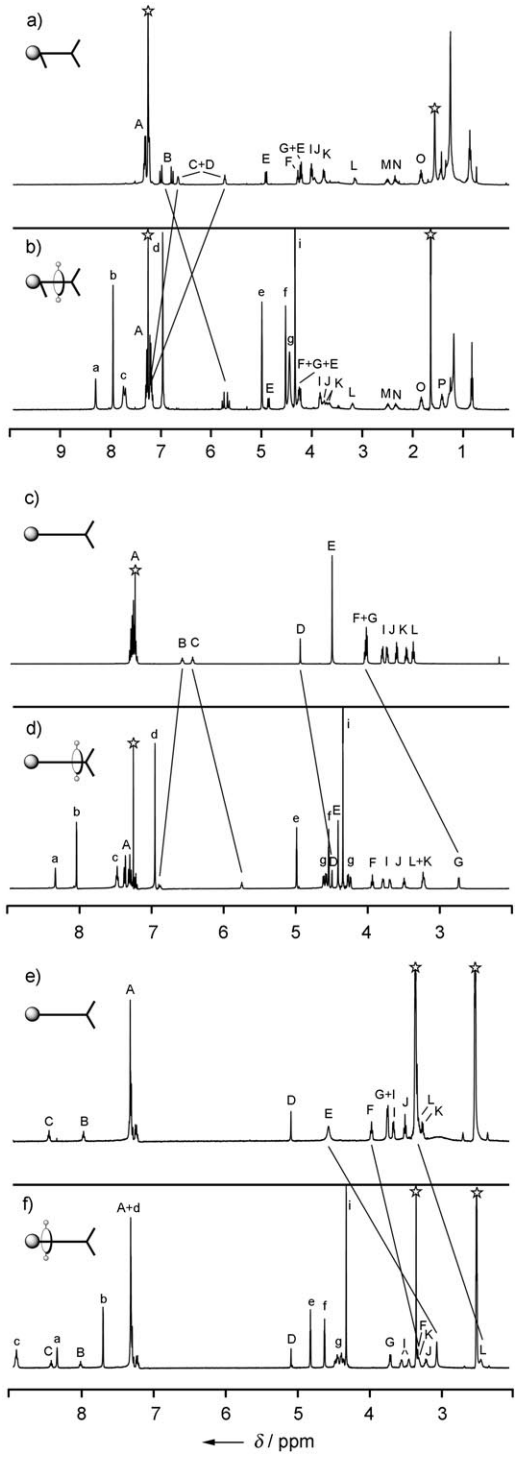

Figure 1. 400 MHz ^{1}H NMR spectra of a) thread **1** in $CDCl_3$, b) rotaxane **2** in $CDCl_3$, c) thread **4** in $CDCl_3$, d) rotaxane **5** in $CDCl_3$, e) thread **4** in $[D_6]$DMSO, f) rotaxane **5** in $[D_6]$DMSO. The peaks highlighted with stars correspond to residual solvent.

polarities between those of $CDCl_3$ and DMF. However, weakening of the hydrogen bonds by a consecutive incremental increase of the polarity increases the shuttling rate[7] and promotes the formation of **5B**. Even if shuttling is rapid on the NMR timescale (ca. 10^{-3} s), this effect is observable in the consecutive deshielding of the peptidic protons G upon increasing the polarity of the medium ($\Delta\delta_G$ (ppm) $CD_2Cl_2 = -1.3$; $CDCl_3 = -1.3$; $[D_8]$THF $= -1.0$; CD_2Cl_2–$[D_2]$HFIP (1:1) $= -0.9$; $[D_7]$DMF $= -0.3$; $[D_6]$DMSO $= -0.1$) (THF = tetrahydrofuran, HFIP = hexafluoroisopropanol).

The redox behavior of the threads (**1** and **4**) and their corresponding rotaxanes (**2** and **5**) was studied in detail by cyclic voltammetry in THF and DMSO solutions (see Table S1 and Figure S3 in the Supporting Information). The voltammograms of thread **1** in THF showed five reduction waves centered on the fullerene (I, II, III, VI, VII) plus two waves centered on the fumaramide template (IV, V). The voltammograms of rotaxane **2** exhibited the same reduction pattern in both solvents and also an extra two-electron anodic reversible peak in the positive potential region (I′) associated with the oxidation of the two equivalent ferrocene moieties on the macrocycle. The fullerene half-wave potentials ($E_{1/2}$) of thread **1** and rotaxane **2** in THF and DMSO are identical, thus corroborating the high complementarity between the macrocycle and the fumaramide, which does not allow any measurable interaction between the macrocycle and the fullerene. The voltammograms of thread **4** in THF exhibited only the first four reduction waves centered on the fullerene (I, II, III, IV). In rotaxane **5**, the same pattern was observed but with two extra waves, which correspond to an additional reduction of the fullerene (V) and to the oxidation of the ferrocene moieties in the macrocycle (I′). Anodic shifts were observed in the $E_{1/2}$ values of the fullerene-centered reduction waves of rotaxane **5** relative to those of thread **4**. This result is indicative of π–π interactions between the fullerene anions and the macrocycle, a consequence of the less efficient binding between the macrocycle and the peptidic template.

Fluorescence spectroscopy is employed both to monitor shuttling and to shed light on the electron donor–acceptor interactions between the photoexcited C_{60} stopper and the ferrocene moieties on the macrocycle. In particular, the fluorescence spectra of **2** and **5** were compared to those of *N*-methylfulleropyrrolidine, **1**, and **4**, in CH_2Cl_2, CH_2Cl_2/HFIP 1:1, and DMF (see Figure S4 in the Supporting Information). While nearly solvent-independent quantum yields of about 6.0×10^{-4} were determined for *N*-methylfulleropyrrolidine, **1**, and **4**, photoexcitation of the ferrocene-C_{60} rotaxanes at 400 nm led to markedly lower quantum yields for **2** and **5** (Table 1).

Table 1: Fluorescence quantum yields for the rotaxane dyads.

Solvent	Rotaxane **2**	Rotaxane **5**
CH_2Cl_2	1.1×10^{-4}	1.3×10^{-4}
CH_2Cl_2/HFIP	0.9×10^{-4}	0.7×10^{-4}
DMF	0.7×10^{-4}	0.3×10^{-4}

The effects of the medium can be deduced by examination of the quantum yields of **2**, since the macrocycle is positioned over the template, irrespective of the solvent used. The quantum yields decrease with increasing hydrogen-bond basicity ($CH_2Cl_2 < CH_2Cl_2$/HFIP < DMF), since larger $-\Delta G°$ values arise for electron-transfer deactivation.[19] A

larger quantum yield is observed for **5** than **2** in CH_2Cl_2. This finding is consistent with the larger relative separation between the electroactive units in CH_2Cl_2, where co-conformation **5A** is mainly present. On the other hand, in CH_2Cl_2/HFIP and DMF,[20] the fluorescence quantum yields of **5** are remarkably lower than in **2** and decrease with increasing hydrogen-bond basicity. Such low quantum yields cannot be rationalized solely on the basis of $-\Delta G°$ values without taking into account the effects derived from molecular shuttling. The reduction in the positional integrity of the macrocycle at the peptidic template, which occurs as the hydrogen bonds are weakened by an incremental increase in hydrogen-bond basicity, causes an increase in the shuttling rate towards the formation of **5B**. This is in strong agreement with the NMR experiments. In fact, the extremely low quantum yields observed in DMF, where co-conformer **5B** exists preferentially, confirm an intimately close donor–acceptor separation.

In time-resolved experiments, the fluorescence lifetimes of **5** (as measured at 710 nm, see Figure S5 in the Supporting Information) are notably shorter than what is typically observed for *N*-methylfulleropyrrolidine, **1**, and **4**. They were estimated to be (0.14 ± 0.02) ns (that is, $(7.1 \pm 0.5) \times 10^9\ s^{-1}$) and 0.11 ± 0.02 ns (that is, $(9.0 \pm 0.5) \times 10^9\ s^{-1}$) in CH_2Cl_2 and CH_2Cl_2/HFIP, respectively, compared to (1.3 ± 0.1) ns (that is, $(7.7 \pm 1.0) \times 10^8\ s^{-1}$) for threads **1** and **4**.[21] These trends are rationalized—in line with previous work—on the basis of intraensemble electron-transfer events to generate a highly energetic radical-ion-pair state. Fluorescence lifetimes of **2** were around 0.1 ns in CH_2Cl_2 and CH_2Cl_2/HFIP.

Additional insights into the electron transfer were obtained from time-resolved transient absorption measurements. Singlet–singlet features of *N*-methylfulleropyrrolidine, **1**, and **4**, were observed, nearly coinciding with the excitation. In the spectral region of interest, that is, visible and near-infrared, two major transitions are discernable: one at 490 and another one at 895 nm. These singlet–singlet features are metastable and subject to an efficient intramolecular intersystem crossing to yield the corresponding triplet excited state. Characteristic of the triplet excited state is a broad transient with a maximum around 700 nm. There is another transient maximum outside the instrumental detection range at 380 nm. Besides the singlet and triplet attributes, the decay of the former is kinetically linked to the formation of the latter (see Figure S6 in the Supporting Information). Overall, we derive intersystem-crossing kinetics of $(7.5 \pm 0.5) \times 10^8\ s^{-1}$.

Similar singlet–singlet characteristics are noted in **2** and **5** at early times after the short laser excitation, namely, during the first few picoseconds. As seen in Figure 2, maxima are located at 490 and 895 nm. Notably, instead of the slow intersystem-crossing dynamics, much faster decays commence with the completed formation of the singlet excited state. Significant kinetic and spectroscopic differences emerge between the C_{60}-ferrocene rotaxanes (**2** and **5**) and the threads (**1** and **4**). Kinetically, the decay of the singlet excited state in **5** occurs within a few tens of picoseconds (namely, $\tau =$ 111 ps in CH_2Cl_2 and $\tau = 80$ ps in CH_2Cl_2/HFIP).[22] These values correspond to deactivation rate constants of 9.0×10^9 and $1.3 \times 10^{10}\ s^{-1}$, which are in strong agreement with the fluorescence-derived values (see above). Lifetimes of 120 and 108 ps were found for **2** in CH_2Cl_2 and CH_2Cl_2/HFIP, respectively, which gives rate constants of 8.3×10^9 and $9.3 \times 10^9\ s^{-1}$.

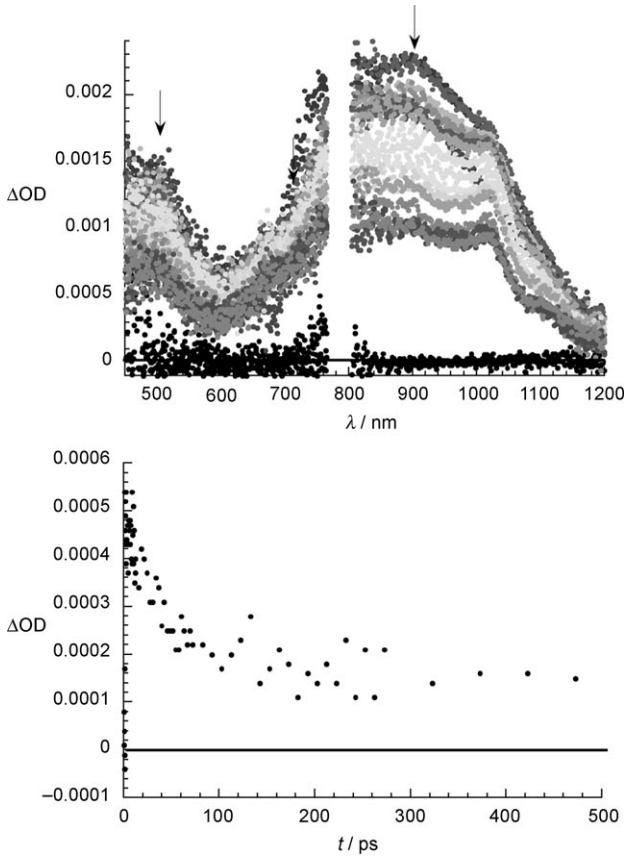

Figure 2. Top: Differential absorption spectra (visible and near infrared) obtained upon femtosecond flash photolysis (387 nm) of rotaxane **5** ($\approx 10^{-5}$ M) in nitrogen-saturated CH_2Cl_2/HFIP solutions. The spectra were measured with several time delays, between 0 and 200 ps, at room temperature (the arrows indicate the singlet features). Bottom: Time–absorption profiles of the spectra shown above (at 490 nm) showing the decay of the singlet excited state.

Spectroscopically, new maxima, with no resemblance to any excited-state feature (C_{60} singlet or triplet), evolve at 505, 650, 895, and 1010 nm.[23] In fact, the peaks at 505, 895, and 1010 nm concur well with the changes observed upon radiolytic or electrochemical one-electron reduction of *N*-methylfulleropyrrolidine (see Figure S7 in the Supporting Information). The feature at 650 nm, on the other hand, resembles that reported for the one-electron oxidation of ferrocene to the ferrocinium ion. Please note that changes associated with the ferrocene-to-ferrocinium oxidation are typically weak ($\varepsilon \approx 500\ M^{-1}cm^{-1}$). The lifetimes of the radical-ion-pair states in CH_2Cl_2 are 8.7 ns (for **2**) and 26.2 ns (for **5**). Again, these values are consistent with the larger relative separation of the electroactive units, which gives longer lifetimes. Addition of HFIP to **5** shortens the lifetime to 13 ns, a consequence—resulting from by weakening the hydrogen bonds—which

causes a decrease in the relative spatial separation between the donor and the acceptor while increasing the shuttling rate.[24] The lifetime for **2** after the addition of HFIP is only reduced to 5.6 ns.

In conclusion, we have demonstrated that submolecular translational motion is a powerful way to modulate/fine-tune the electron-transfer kinetics and, in turn, the lifetime of the radical-ion-pair states. This is achieved in a bistable molecular shuttle through translocation of the ferrocene donors along the fullerene-stoppered thread. The different spatial arrangements of the electroactive units, namely, fullerene and ferrocene, in a series of solvents are consistent with the changes observed in NMR, electrochemical, steady-state, and time-resolved absorption measurements. Moreover, steady-state and time-resolved photophysical measurements centered on the fullerene have shown to be very useful for monitoring fast submolecular motions, such as shuttling.

Received: December 13, 2006
Published online: March 30, 2007

Keywords: electron transfer · fullerenes · molecular shuttles · photosynthesis · rotaxanes

[1] V. Balzani, A. Credi, M. Venturi, *Molecular Devices and Machines*, Wiley-VCH, Weinheim, **2003**.
[2] A. M. Brouwer, C. Frochot, F. G. Gatti, D. A. Leigh, L. Mottier, F. Paolucci, S. Roffia, G. W. H. Wurpel, *Science* **2001**, *291*, 2124 – 2128.
[3] V. Balzani, M. Clemente-Leon, A. Credi, B. Ferrer, M. Venturi, A. H. Flood, J. F. Stoddart, *Proc. Natl. Acad. Sci. USA* **2006**, *103*, 1178 – 1183.
[4] H. R. Tseng, S. A. Vignon, J. F. Stoddart, *Angew. Chem.* **2003**, *115*, 1529 – 1533; *Angew. Chem. Int. Ed.* **2003**, *42*, 1491 – 1495.
[5] A. Altieri, F. G. Gatti, E. R. Kay, D. A. Leigh, D. Martel, F. Paolucci, A. M. Z. Slawin, J. K. Y. Wong, *J. Am. Chem. Soc.* **2003**, *125*, 8644 – 8654.
[6] J.-P. Sauvage, *Chem. Commun.* **2005**, 1507 – 1510.
[7] A. S. Lane, D. A. Leigh, A. Murphy, *J. Am. Chem. Soc.* **1997**, *119*, 11092 – 11093.
[8] T. Da Ros, D. M. Guldi, A. F. Morales, D. A. Leigh, M. Prato, R. Turco, *Org. Lett.* **2003**, *5*, 689 – 691.
[9] D. A. Leigh, M. A. F. Morales, E. M. Perez, J. K. Y. Wong, C. G. Saiz, A. M. Z. Slawin, A. J. Carmichael, D. M. Haddleton, A. M. Brouwer, W. J. Buma, G. W. H. Wurpel, S. Leon, F. Zerbetto, *Angew. Chem.* **2005**, *117*, 3122 – 3127; *Angew. Chem. Int. Ed.* **2005**, *44*, 3062 – 3067.
[10] A. Mateo-Alonso, G. Fioravanti, M. Marcaccio, F. Paolucci, D. C. Jagesar, A. M. Brouwer, M. Prato, *Org. Lett.* **2006**, *8*, 5173 – 5176.
[11] A. M. Elizarov, S. H. Chiu, J. F. Stoddart, *J. Org. Chem.* **2002**, *67*, 9175 – 9181.
[12] C. M. Keaveney, D. A. Leigh, *Angew. Chem.* **2004**, *116*, 1242 – 1244; *Angew. Chem. Int. Ed.* **2004**, *43*, 1222 – 1224.
[13] A. Mateo-Alonso, A. M. Prato, *Tetrahedron* **2006**, *62*, 2003 – 2007.
[14] M. Maggini, G. Scorrano, M. Prato, *J. Am. Chem. Soc.* **1993**, *115*, 9798 – 9799.
[15] M. Prato, M. Maggini, *Acc. Chem. Res.* **1998**, *31*, 519 – 526.
[16] F. G. Gatti, D. A. Leigh, S. A. Nepogodiev, A. M. Z. Slawin, S. J. Teat, J. K. Y. Wong, *J. Am. Chem. Soc.* **2001**, *123*, 5983 – 5989.
[17] A. Altieri, G. Bottari, F. Dehez, D. A. Leigh, J. K. Y. Wong, F. Zerbetto, *Angew. Chem.* **2003**, *115*, 2398 – 2402; *Angew. Chem. Int. Ed.* **2003**, *42*, 2296 – 2300.
[18] A. Mateo-Alonso, G. M. A. Rahman, C. Ehli, D. M. Guldi, G. Fioravanti, M. Marcaccio, F. Paolucci, M. Prato, *Photochem. Photobiol. Sci.* **2006**, *5*, 1173 – 1176.
[19] The energies of the radical-ion-pair states of **2** and **5** were estimated by adding the first reduction potential of the electron acceptor and the first oxidation potential of the electron donor (reported in Table S1 in the Supporting Information). The values are 1.31 and 1.05 eV in THF and DMSO, respectively, for both **2** and **5**. However, only when adding a correction term (D. M. Guldi, M. Maggini, E. Menna, G. Scorrano, P. Ceroni, M. Marcaccio, F. Paolucci, S. Roffia, *Chem. Eur. J.* **2001**, *7*, 1597 – 1605), which accounts for ion-pair electrostatic interactions at the different donor–acceptor distances, do the values start to differ (from 1.1 to 0.9 eV for **2** and from 1.0 to 0.6 eV for **5**) by increasing the solvent polarity from CH_2Cl_2 to DMF.
[20] Quantum yields similar to those observed in DMF were found for **5** in HFIP (0.3×10^{-4}) and DMSO (0.2×10^{-4}).
[21] The fluorescence lifetime in DMF is likely to be outside the detection range of our apparatus (0.10 ns).
[22] The inherent photochemistry associated with DMSO and the instability of DMF solutions under typical radiolysis conditions did not allow reliable data to be recorded in these solvents. However, CH_2Cl_2/HFIP solutions present a greater stability. Even if the positional discrimination towards **5B** in CH_2Cl_2/HFIP is less well observed by NMR spectroscopy because of a slower timescale (10^{-3} s), the effects of fast positional exchange have a big impact on time-dependent absorption spectroscopic techniques because of the shorter timescales (10^{-15}, 10^{-12}, 10^{-9} s) and the enhanced sensitivity.
[23] **5**: in CH_2Cl_2, CH_2Cl_2–HFIP, HFIP, and DMF; **2**: in CH_2Cl_2, CH_2Cl_2/HFIP, and HFIP.
[24] Charge recombination kinetics, which are located in the inverted region of the Marcus parabola, also contribute to the shorter lifetimes.

